

# Generalized Time-Domain Index Modulation with A Low Complexity Detection Method

Rongfang Zhang, Weikai Xu, Xiangming Cai, Lin Wang

Dept. of Information and Communication Engineering, Xiamen University, Fujian 361005, China  
xweikai@xmu.edu.cn

**Abstract**—SC-based index modulation (SC-IM) is a recently developed communication scheme that uses the optimal high complexity maximum likelihood (ML) detection algorithm at receiver. In this paper, we propose a single-carrier-based generalized time-domain index modulation (GTD-IM) scheme whose receiver employs a square-law envelope detector (SLED) to detect the active indices. Through analyses and simulations, we find that this system can achieve approximate energy efficiency and error performance of SC-IM with a lower implementation complexity.

**Index Terms**—SC-IM, ML detection, SLED, energy efficiency, detection complexity, multipath Rayleigh channel.

## I. INTRODUCTION

Compared with the traditional modulation scheme, index modulation (IM) is a novel modulation, which is able to convey additional information by a new extended third dimension constellation based on conventional 2-D signal constellation. The IM has been used in the spatial [1], [2], the frequency [3], [4], [5], the code [6], [7] and the space-time [8], [9] domains to achieve both high data rate and energy efficiency. In [1], the spatial modulation (SM) was put forward as a promising multiple-input multiple-output (MIMO) transmission technique, which could solve the inter-channel interference (ICI) problem at receiver and the synchronization of multiple transmit antennas. In SM system, the information is conveyed not only by the conventional constellation symbols such as  $M$ -ary phase shift keying ( $M$ -PSK) or  $M$ -ary quadrature amplitude modulation ( $M$ -QAM), but also by the selected transmit antenna indices of an MIMO system. Inspired by the concept of SM, the orthogonal frequency division multiplexing with index modulation (OFDM-IM) has been proposed as a novel multi-carrier transmission scheme for frequency selective fading channels [5]. The motivation behind this new concept is to improve bit error ratio (BER) performance and energy efficiency over conventional OFDM. Similar to the bit mapping of SM, the incoming information bits stream is divided into two parts, one part of information bits is used in conventional modulation, other part acts as subcarrier index mapped bits, which is carried by the specific legitimate combination of the activated subcarrier indices. Compared with traditional OFDM, OFDM-IM divides all the sub-carriers into many sub-blocks, and the index selection bits determine the activated sub-carrier in each sub-block. Meanwhile, the active sub-carriers are used to transmit  $M$ -ary constellation symbols and the remaining sub-carriers are

inactive. As a result, it has been proved that OFDM-IM shows better BER performance than classical OFDM, especially in the low-rate scenario. However, this system still has the same flaws with OFDM, such as high peak-to-average power ratio (PAPR).

In terms of system complexity, the OFDM-IM scheme is hard to implement based on the high-complexity maximum-likelihood (ML) detection, which performs a joint search by considering all possible active sub-carrier combinations and symbols [5]. As a result, its exponentially growing decoding complexity makes this scheme impractical for large combination values. Hence, the near-optimal log-likelihood ratio (LLR) detection strategy is proposed for high number of sub-carriers, but it does not include the set of all legitimate sub-carrier activation combinations [5]. Subsequently, a modified frequency index modulation (FIM) scheme is proposed in [10], which is simpler than approach of [5]. In the receiver of this system, a low complexity square-law envelope detector (SLED) is used in each sub-frame to determine the most likely active subcarrier and the corresponding constellation symbols. The proposed detection method makes this OFDM-IM system as an excellent candidate for wireless sensor applications, since it has achieved lower complexity and lower energy consumption in frequency selective fading channels.

Furthermore, according to [11], the OFDM-IM scheme typically exhibits a high PAPR and a high power-backing off under the idealized simplifying assumption of Gaussian distribution incoming symbols, which are nearly identical with the OFDM systems. It is obvious that the limitations and inherent problems of OFDM are difficult to avoid. In response to these problems, a single-carrier with frequency-domain equalization systems (SC-FDE) is proposed in [12], which is highly similar to OFDM system. SC-FDE system has two main appealing advantages over OFDM, namely, lower PAPR and reduced sensitivity to carrier frequency errors. As a result, SC-FDE can be considered as a promising broadband wireless technique for high-speed wireless communications systems. In [13], IM has been combined with SC-FDE. SC-FDE with IM (SC-IM) can convey additional information by activating a set of indices of time-domain symbols in sub-frames at the transmitter, and employ the ML detection to detect transmitted bits at the receiver. But ML detection has an exponentially growing decoding complexity, there's still a room to improve performance of the FDE-aided SC-IM.

In this paper, we propose a modified FDE-aided SC-IM,

which is referred to as generalize time-domain index modulation scheme (GTD-IM). In this scheme, we apply the SLED to detect activated indices of time-domain symbols in each sub-frame at receiver, which has a lower complexity than that of the approach in [13]. By employing combinational method to select indices at transmitter and receiver, the SLED method is generalized to any number of active symbols. In a word, the proposed scheme is not only capable of attaining a significantly lower PAPR than OFDM-IM, but also implementing a comparable low detection complexity compared with SC-IM.

The rest of the paper is organized as follows. The next section presents the proposed system model. Section III analyzes energy efficiency and system complexity. Numerical simulations are presented in Section IV. Section V concludes the paper.

## II. SYSTEM MODEL

### A. The Transmitter

Based on principle of the FDE-aided SC-IM [13] and the SLED, we propose the GTD-IM system. The structure of the proposed GTD-IM system is illustrated in Fig. 1.

In the proposed GTD-IM system, each frame consists of a  $N$ -length data symbols  $\mathbf{s} = [s_1, s_2, \dots, s_N]^T \in \mathbb{C}^N$  and a  $J$ -length cyclic prefix (CP), where  $N$  is the number of GTD-IM slot times to be mapped, i.e., the size of the FFT. As seen from Fig. 1, the transmitter of GTD-IM system divides a total of  $m$  information bits into  $L$  equal length sub-frame which contains  $p$  bits, i.e.,  $m = pL$ . Thus, the transmitted data symbol is denoted by  $\mathbf{s} = \{\mathbf{x}(1)^T, \mathbf{x}(2)^T, \dots, \mathbf{x}(L)^T\}^T$ , where  $\mathbf{x}(j)^T = \{s_1(j), s_2(j), \dots, s_n(j)\} \in \mathbb{C}^n (j = 1, 2, \dots, L)$  represents the  $j^{th}$  sub-frame. According to [13], each sub-frame spans  $n$  symbol durations, i. e.,  $N = Ln$ .

Similar to OFDM-IM, the incoming  $p$ -bits of each sub-frames are split into two parts, the first  $p_1$  bits is mapped to the indices of active symbols, and the second  $p_2$  bits is used to modulate  $M$ -ary constellation symbol such as  $M$ -PSK or  $M$ -QAM, i.e.,  $p = p_1 + p_2$ . Following the principle of IM, the transmitter picks out  $k$  active indices of slots from  $n$  available slots to carry  $k$   $M$ -ary constellation symbols (i.e., for  $j^{th}$  sub-frame, there is  $\mathbf{s}_*(j) = \{s_*^1, s_*^2, \dots, s_*^k\}$ , where  $s_*^\beta \in \mathcal{S}$  and  $\beta=1, 2, \dots, k$ ) in each sub-frame. And the selected indices are given by  $\mathbf{I}(j) = \{i_1, i_2, \dots, i_k\}$  where  $i_\beta \in [1, 2, \dots, n]$ ,  $|\mathbf{I}(j)| = k$ . As for the methods used to select indices in proposed scheme, we will present two different mapping methods in subsection II-B.

Meantime, the remaining  $(n - k)$  slots are set to zero that do not be used to transmit symbols. Fig. 1 illustrates the case where  $\mathbf{b}_j^{p_1} = [0 \ 1]$  determines that the second symbol is activated to carry the constellation symbols mapped by  $\mathbf{b}_j^{p_2} = [1 \ 0]$ . In a word, we can carry the total number of  $p_1 = \lfloor \log_2 C(n, k) \rfloor$  information bits through the positions of the active indices of each GTD-IM sub-frame, where  $\lfloor \cdot \rfloor$  is the floor operator. On the other hand, the total number of information bits carried by  $M$ -ary signal constellation symbols is given by  $p_2 = k \log_2 M$ . Consequently, for each GTD-IM

frame, there are  $m$  information bits to be transmitted,

$$m = pL = (p_1 + p_2)L = (\lfloor \log_2 C(n, k) \rfloor + k \log_2 M)L. \quad (1)$$

In the  $j^{th}$  sub-frame, we have

$$\mathbf{x}^i(j) = \begin{cases} 0, & i \notin I, \\ s_*^\beta(j), & i \in I. \end{cases} \quad (2)$$

where  $i \in [1, 2, \dots, n]$ . To normalize the signal constellation to a unit average power, the  $k$  non-zero  $M$ -ary signal constellation symbols are scaled by  $\sqrt{n/k}$ , i. e.,  $(\sum_{g=1}^n |x^g(j)|^2 / n) = 1$ .

And the transmitted sub-frame  $\mathbf{x}(j)$  has an actual energy  $E_x = E[\mathbf{x}(j)\mathbf{x}(j)^*] = p_2 E_b$  where  $E_b$  is the bit energy. As the system uses IM to transmit additional information bits which does not occupy bit energy, we need to recalculate the equivalent bit energy  $E_{eb}$  which represents the equivalent energy consumed per transmitted bit. As a result, it makes a fair comparison between the proposed system and other traditional systems. The relationship between this equivalent system bit energy and the physically modulated bit energy is described as,

$$E_{eb} = \frac{p_2}{p_1 + p_2} E_b = \frac{p_2}{p} E_b. \quad (3)$$

The normalized throughput of the proposed GTD-IM system is given by

$$R = \frac{N}{N+J} \cdot \frac{\lfloor \log_2 C(n, k) \rfloor + k \log_2 M}{n} [\text{bit/symbol}], \quad (4)$$

where the coefficient  $\frac{N}{N+J}$  represents the rate loss from CP insertion.

### B. The Receiver

The diagram of the GTD-IM receiver is shown in Fig. 1. Let the  $(N+J)$ -length received signal at the receiver be denoted by  $\mathbf{r} = [r_{N-J+1}, r_{N-J+2}, \dots, r_N, r_1, r_2, \dots, r_N]^T \in \mathbb{C}^{N+J}$  in each frame. And the channel can be expressed by  $\nu$  channel impulse response (CIR) coefficients that are circularly symmetric complex Gaussian random variables subject to  $\mathcal{CN}(0, \frac{1}{\nu})$  distribution. In order to eliminate inter-symbol interference (ISI), it is ensured that the CIR length of  $\nu$  is less than the CP length of  $J$ . After receiving the signal, the receiver performs the operation of removing the CP from  $(N+J)$ -length received signal. The following operation is to perform FFT on the  $N$ -length received signals, which is represented by

$$\mathbf{r} = [r_1, r_2, \dots, r_N]^T = \mathbf{h} \otimes \mathbf{s} + \mathbf{z}, \quad (5)$$

where  $\otimes$  is convolution operator and  $\mathbf{z} = [z_1, z_2, \dots, z_N]^T \in \mathbb{C}^N$  is an independent additive white Gaussian noise (AWGN) vector, which are given by complex-valued Gaussian random variables with  $\mathcal{CN}(0, N_0)$ . By the FFT, the signal is transformed from time domain to frequency domain, so that the received data signals can be equalized by the FDE algorithm. In fact, this is the frequency domain analysis of the received signal.

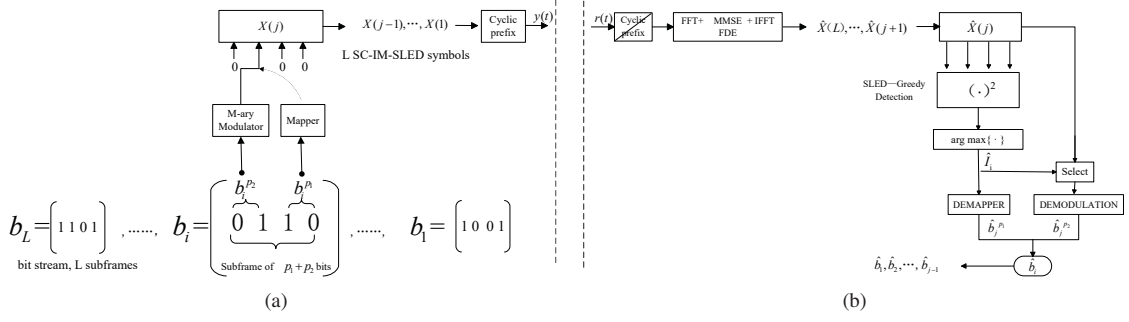


Fig. 1: The block diagram of GTD-IM communication system. (a) Transmitter, (b) Receiver.

Let  $\mathbf{h}$  denotes the channel impulse response and  $\mathbf{H}$  denotes its Fourier transform, i.e., the channel transfer function. Then in frequency domain, we have

$$r^i(j) = \begin{cases} Z^i(j), & i \notin I(j) \\ H^i(j)s_*^\beta(j) + Z^i(j), & i \in I(j) \end{cases} \quad (6)$$

in the  $j^{th}$  sub-frame, where  $\mathbf{Z}$  is the Fourier transform of  $z$ . Equalization of the channel needs to be applied at the FFT output in the receiver, and the received signal  $r^i(j)$  needs to be multiplied by a complex coefficient  $W_{ZF}^i(j) = 1/H^i(j)$ , which is the zero-forcing (ZF) criterion to completely eliminate ISI even though the noise is also amplified. In order to better reduce the combined effects of ISI and additive noise, the equalizer coefficients can be optimized under the MMSE criterion [12]. This criterion requires that the mean square error between the decision value and the expected value is minimal, and the coefficient of the MMSE equalizer is

$$W_{MMSE}^i(j) = \frac{H^i(j)^*}{|H^i(j)|^2 + \sigma_n^2/\sigma_a^2}, \quad (7)$$

where  $\sigma_n^2$  is the variance of additive noise and  $\sigma_a^2$  is the variance of the transmitted data symbols. When  $\sigma_n^2=0$ , the MMSE criterion reduces to the ZF criterion.

Finally, after performing IFFT operations on the frequency domain equalized signal, the time domain signal is estimated as  $\hat{\mathbf{s}} = \{\hat{\mathbf{x}}(1)^T, \hat{\mathbf{x}}(2)^T, \dots, \hat{\mathbf{x}}(L)^T\}^T$ . To attain the all incoming bits, the active index  $\hat{I}(j)$  should be detected by some detection methods, and then the selected constellation symbols with  $\hat{I}(j)$  are demodulated in each sub-frame. We will refer to these detection methods in the next subsection.

### C. The Detection Algorithm

To detect the indices of the active symbols and the corresponding information symbols with  $\mathbf{r} = [r_1, r_2, \dots, r_N]^T \in \mathbb{C}^N$  is main task of the receiver. After getting the signal symbols to be estimated, the next step is to detect the corresponding data bits.

1) *ML Detector*: According to [5], the ML detector is used to detect the received signals, which considers all possible sub-frame realizations, i.e.,  $I(j)$  has  $c = 2^{p_1}$  possible realizations. This straightforward solution makes a joint decision on

the active indices and the constellation symbols for each sub-frame by searching all possible symbol index combinations and the signal constellation points by minimize the following metrics:

$$(\hat{I}(j), \hat{\mathbf{s}}(j)) = \arg \min_{I(j), \mathbf{s}(j)} \sum_{\beta=1}^k |\hat{\mathbf{x}}^{i,j,\beta}(j) - \mathbf{s}_*^\beta(j)|^2. \quad (8)$$

The total computational complexity of the ML detector can be represented by  $\mathcal{O}(cM^k)$  per sub-frame since  $I(j)$  and  $\mathbf{s}_*(j)$  have  $c$  and  $M^k$  different realizations, respectively. As a result, since the decoding complexity increases exponentially, when  $c$  and  $k$  become large, such an ML detector will become unsuitable.

2) *SLED Detector*: In order to make the proposed scheme more feasible, we provide a novel low-complexity detector at the receiver, i.e., SLED. The SLED is used to estimate the active symbol indices in the  $j^{th}$  sub-frame. Unlike the FIM system in [10], the proposed system is generalized to any number  $k$  of active symbols between 1 and  $(n-1)$ . The receivers detection task is mainly divided into two processes where indices of the active symbols and corresponding data symbols are detected separately. Firstly, the proposed detection method needs to detect the received signal energy on each symbol in order to find the active symbol indices. Thus, the vector  $\hat{\mathbf{x}}(j)$  is input into an energy detector to get  $n$  decision variables, we have

$$p^i(j) = \begin{cases} |W_{MMSE}^i(j)Z^{i'}(j)|^2, \\ |W_{MMSE}^i(j)H^i(j)s_*^\beta(j) + W_{MMSE}^i(j)Z^i(j)|^2. \end{cases} \quad (9)$$

Among the measured received signal energies, the SLED choose the  $k$  greatest received energies as the estimate of active symbols, which means it is more probable that these  $k$  corresponding indices is selected by the index selector at the transmitter. Thus, the receiver can extract  $p_1$  mapped bits by estimating the active symbol index  $\hat{I}(j)$ . Secondly, according to the estimated  $k$  indices, the receiver can determine  $k$  slots which transmit the data symbols at transmitter. Then followed by a conventional  $M$ -ary constellation symbol demodulator, the receiver extracts the remaining  $p_2$  modulated bits from  $\hat{\mathbf{x}}(j)$ .

TABLE I: A Look-up table example for  $n = 4, k = 2$  and  $c = 4$

Bits	Indices	Sub-frames
0 0	2,1	$[s_*^X, s_*^Z, 0, 0]^T$
0 1	3,1	$[s_*^X, 0, s_*^Z, 0]^T$
1 0	3,2	$[0, s_*^X, s_*^Z, 0]^T$
1 1	4,1	$[s_*^X, 0, 0, s_*^Z]^T$

#### D. The Index Selection

In this subsection, we will discuss index selector and index de-mapper, then give different implementations of them. To pick  $k$  active indices out of  $n$  available symbols, the index selector has  $C(n, k)$  possible candidates for each sub-frame.

Considering the complexity and feasibility of the GTD-IM system, two mapping methods are presented.

1) *Look-Up Table Method*: As stated in subsection II-A, we have  $n$  symbols for each sub-frame, which means that  $I(j)$  has  $c = 2^{p_1}$  possible realizations. This means that the size of the look-up table is  $c$  in this mapping method, which is created at both transmitter and receiver sides. At the transmitter, the look-up table is used as a mapping tool to provide a one-to-one mapping relationship between the incoming  $p_1$  bits and the active indices combination for each sub-frame. At receiver, in the case of having an estimated indices combination, we need to traverse the entire look-up table space to get the corresponding bits. An example of a look-up table can be seen in Table 1 for  $n = 4, k = 2$  and  $c = 4$ , where  $s_*^X, s_*^Z \in \mathcal{S}$ . Considering  $C(n, k) = 6$  in this case, the method has to give up two combinations.

Because of this methods practicality, whether the receiver of the GTD-IM system uses ML detector or SLED, this method is universal. On the one hand, when this method is employed in the ML detector, the receiver will know a series of possible indices based on this look-up table, which helps the ML detector to consider all possible sub-frame realizations. On the other hand, in order to reduce the decoding complexity of the exponential growth of the actual ML decoder, the SLED can be operated in conjunction with a look-up table. By using the SLED for each sub-frame, the receiver makes a decision on the set of active indices by choosing the set with the  $k$  greatest received energies. Next, the detector traverse the entire table to find the corresponding  $p_1$  mapping bits, and finally demodulated the corresponding  $M$ -ary constellation symbols. However, the size of look-up table grows with the number of incoming bits, the use of look-up tables becomes not feasible when  $k$  and  $n$  are large. Therefore, the following method is proposed.

2) *Combinatorial Method*: This method is mentioned in [14], [15], and is applied in [15]. According to the above literatures, the combinational number system provides an one-to-one mapping between natural numbers and  $k$ -combinations, for all  $n$  and  $k$ . This means that it maps a natural number into a strictly decreasing sequence  $Seq = \{w_k, w_{k-1}, \dots, w_1\}$ , where  $w_k > w_{k-1} > \dots > w_1 \geq 0$ . In other words, for any  $n$  and

$(0 < k < n)$ , we can represent all  $Z \in [0, C(n, k) - 1]$  with a sequence  $Seq$  of length  $k$ , which takes elements from the set  $\{0, 1, \dots, n - 1\}$  by the following equation

$$Z = \sum_{i=1}^k C(w_i, i), \quad (10)$$

where  $C(m, n)$  is the combinational number.

The lexicographically ordered  $Seq$  sequences for all  $n$  can be found by the algorithm as follows: firstly, choose the maximal  $c_k$  satisfying  $C(c_k, k) \leq Z$ , and then remove  $c_k$  from the set  $\{0, 1, \dots, n - 1\}$ ; secondly, choose the maximal  $c_{k-1}$  satisfying  $C(c_{k-1}, k-1) \leq Z$  and so on [15]. Applying this algorithm to our proposed scheme, for each frame, we can first convert the binary incoming bits to a decimal number in the index selector. And then the combinatorial algorithm is applied to the decimal number to get a  $Seq$  sequence. Then the sequence  $Seq + 1$  gives us the active indices we need. At the receiver, we can convert the active indices obtained by the index detection to a decimal number  $\hat{Z}$  using (10). After determining active indices by using the SLED, we use this method to demodulate the  $p_1$  mapped bits for larger  $c$  to avoid look-up tables. However,  $\hat{Z} \geq c$  may occur since  $c$  is less than  $C(n, k)$ , which can give a catastrophic result at the receiver. Thus, if  $\hat{Z} \geq c$ , then  $\hat{Z} = c - 1$ . Although this practice may cause a little error, we use this detector for higher  $k$  and  $n$ .

### III. ENERGY EFFICIENCY AND COMPLEXITY

In the section, the energy efficiency and complexity of the proposed GTD-IM system are analyzed.

#### A. Energy Efficiency

As we know, IM achieves higher energy efficiency by considering the indices of the activated symbols as a new dimension to transmit information bits in addition to the conventional modulation schemes. In other words, the system actually only transmits conventional modulation symbols. However, due to the role of the indices, the information carried by the receiver is actually more than the conventional modulation symbols.

In the proposed GTD-IM systems, only  $p_2 L$  bits from the total  $(p_1 + p_2)L$  are directly transmitted by the  $M$ -ary symbols, and the index of the transmitted symbols carries  $p_1 L$  bits. Considering that each modulated bit requires an energy of  $E_b$  to be transmitted, the percentage of the energy saving per sub-frame in the proposed GTD-IM is given by

$$E_{saving} = (1 - E_{eb})\% = \left(1 - \frac{p_2}{p_1 + p_2}\right) E_b\% \\ = \left(1 - \frac{1}{p_1/p_2 + 1}\right) E_b\%. \quad (11)$$

Since  $p_1 = \lfloor \log_2 C(n, k) \rfloor$  and  $p_2 = k \log_2 M$ , the saved energy is affected by the modulation order  $M$ , the length of sub-frame  $n$  and the number of active symbols  $k$ . It is worth mentioning that when the modulation order and the number of symbols are fixed, an augmentation in the number of activated symbols can reduces energy efficiency.



In [13], we can know that the SC-IM scheme also achieves the same energy efficiency, i.e.,  $E_{\text{saving}} = \left(1 - \frac{1}{p_1/p_2+1}\right) E_b\%$ . It means that the two systems are similar in terms of energy efficiency.

#### B. System Complexity

The proposed GTD-IM system uses SLED instead of ML detection in order to achieve low complexity. The complexity is evaluated by the number of operations required. Firstly, since the GTD-IM uses IFFT and FFT operations with a length of  $N$ , the computational complexity will be  $\mathcal{O}_{\text{FFT/IFFT}} \sim \mathcal{O}(2N \log_2 N)$ . Secondly, after SLED multiplies the vector  $\hat{\mathbf{x}}(j)$  by its complex conjugate, the resulting sequence is sorted using a quick sort algorithm. Then the  $k$  greatest values are chosen as the estimate of the active indices. Therefore, the computational complexity of this part is simplified  $\mathcal{O}_{\text{SLED}} \sim \mathcal{O}(n \log_2 n)$  per sub-frame. Finally, the computational complexity of a modulator and a demodulator will be  $\mathcal{O}_{\text{Mod/Demod}} \sim \mathcal{O}(3p_2 - 1)$  per active symbol [10]. In total, the complexity of the GTD-IM system would be expressed as,

$$\mathcal{O}_{\text{GTD-IM}} = \mathcal{O}_{\text{FFT/IFFT}} + L\mathcal{O}_{\text{SLED}} + kL\mathcal{O}_{\text{Mod/Demod}}. \quad (12)$$

In order to more intuitively understand the advantages of SLED over ML detection, we compare the complexity of GTD-IM to that of conventional SC-IM in the same modulation order. In the latter, similarly  $k$  out of  $n$  symbols are activated, but the complexity of the ML detector is  $\mathcal{O}_{\text{MLD}} \sim \mathcal{O}(2^{p_1} M^k)$ , which is exponentially growing. Therefore, total complexity is

$$\mathcal{O}_{\text{SC-IM(ML)}} = \mathcal{O}_{\text{FFT/IFFT}} + L\mathcal{O}_{\text{MLD}} + kL\mathcal{O}_{\text{Mod/Demod}}. \quad (13)$$

In recent years, in order to reduce the decoding cost of SC-IM, a special log-likelihoodratio(LLR) detector has been introduced [16]. The computational complexity of each LLR is  $\mathcal{O}_{\text{LLR}} \sim \mathcal{O}(M)$ . As a result, the complexity will be

$$\mathcal{O}_{\text{SC-IM(LLR)}} = \mathcal{O}_{\text{FFT/IFFT}} + nL\mathcal{O}_{\text{LLR}} + kL\mathcal{O}_{\text{Mod/Demod}}. \quad (14)$$

### IV. SIMULATION RESULTS AND COMPARISONS

In this section, computer simulations are carried out to evaluate the performance of the proposed systems in the presence of frequency selective channels described in Section II. Then we compare the performance of GTD-IM to SC-IM system. Finally, we study the complexity analyses for the proposed system. In all simulations, we assumed the following system parameters:  $N = 256$  and  $J = 32$ .

#### A. Performance of GTD-IM

Figure 2 shows the BER performance of GTD-IM and SC-IM schemes under different CIR length of frequency selective fading channels. The IM parameters were set to  $(n, k, M) = (4, 1, 4)$  for the GTD-IM and SC-IM schemes. Then, we can observe that different degrees of the multipath diversity could be extracted when the CIR length is given by  $\nu = 1, 2$  and

4. It is obvious that increasing  $\nu$  values created the growth of the diversity gain, and both schemes achieved approximate performance.

Consider the case when, for a given  $n$ , the number of activated symbols per sub-frame  $k$  tends to grow up to  $(n - 1)$ . In Fig. 3, we investigated the effects of  $k$  on the error performance of the GTD-IM and SC-IM schemes using QPSK with  $n = 4$  and  $\nu = 4$ . As seen from this figure, with the decreasing of  $k$ , the error performance of the GTD-IM and SC-IM schemes improved, which was achieved at the expense of the reduction in the transmission rate.

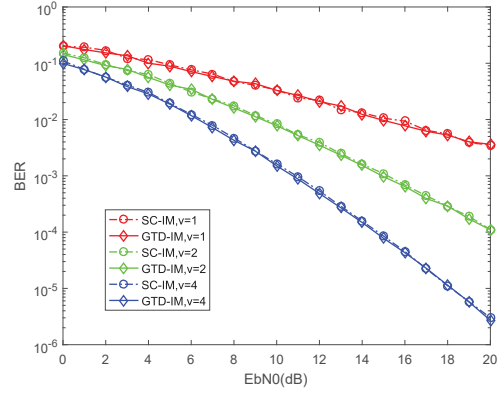


Fig. 2: Performances comparison of the proposed system and SC-IM system with the CIR length  $\nu = 1, 2$  and 4,  $(n, k, M) = (4, 1, 4)$ .

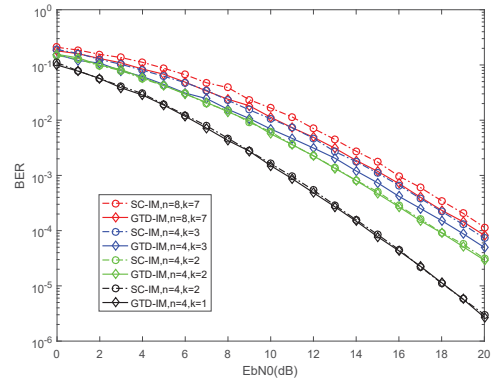


Fig. 3: Performances comparison of the proposed system and SC-IM system with various length of sub-frame  $n$  and activated symbols  $k$  per sub-frame,  $M = 4$ .

From the above two figures, we can see that the GTD-IM and SC-IM schemes exhibit exactly the same BER performance, as expected. As mentioned previously, the SC-IM scheme which uses ML detection, employs a look-up table, while the GTD-IM scheme with a low complexity SLED, uses the combinatorial method. It is interesting that the SLED, which is actually a near-ML detection, achieves the same BER performance as that of the ML detection. Even at  $k = n - 1$ ,

as the Fig.3 shows, the performance of GTD-IM scheme outperformed the SC-IM scheme when  $n = 4, k = 3$  and  $n = 8, k = 7$ . This can be attributed to the fact that the number of unused combinations out of the all possible index combinations is equal to 0 for  $k = n - 1$ . In this case, it is more easy to choose  $k = n - 1$  correct index symbols from  $n$ , which is equivalent to the difficulty of the case when  $k = 1$ . However, compared to case of  $k = 1$ , the increasing number of modulated symbols cause the deterioration of BER performance at  $k = n - 1$ .

### B. Complexity Analysis

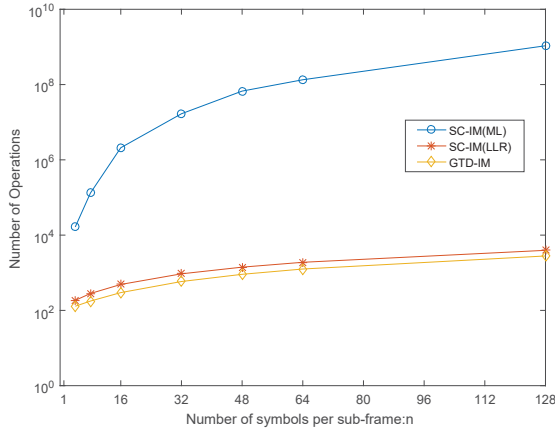


Fig. 4: Complexity comparison of the proposed GTD-IM, SC-IM(ML) and SC-IM(LLR) systems using a number of sub-frame  $L = 1$  and FFT-length  $N = nL$ .

In this subsection, we show the computational complexity of the GTD-IM and the SC-IM using the ML and LLR detection. We compare the complexity of these three schemes under the same parameters, i.e., fixed transmission rate and transmission condition. Clearly, due to the exponential increase in the complexity of ML detection, the computational complexity of the SC-IM using ML detection is higher than the others. As for the LLR detection, we observe that its complexity is  $\mathcal{O}(nM)$  whereas the complexity of the GTD-IM is  $\mathcal{O}(n \log_2 n)$  for each sub-frame. In fact we have  $\mathcal{O}_{\text{GTD-IM}} \leq \mathcal{O}_{\text{SC-IM(LLR)}} \leq \mathcal{O}_{\text{SC-IM(ML)}}$ .

Figure 4 depicts the computational complexity based on (12), (13) and (14) that represent the complexity of these systems, by fixing these data such as  $k = 3, L = 1$  and  $M = 16$ . As the number of symbols increases,  $n > 3$ , in terms of complexity, the proposed scheme is far superior to the ML detection, and slightly better than the LLR detection.

### V. CONCLUSIONS

In this paper, we proposed a generalized time-domain index modulation (GTD-IM) scheme which used a low complexity detection at receiver. In the proposed scheme, the indices were detected by finding all possible slots with the greatest received

energy which avoids the exhaustive search of the ML detection. Compared to ML detection, simulations showed that the proposed detection method exhibited negligible losses of BER performance. In terms of complexity, analyzed results showed that this proposed scheme had great advantages compared to SC-IM with ML detection. Although the complexity of the SLED and LLR detection is similar, the SLED is easier to implement than the LLR detection. In a word, the GTD-IM scheme can be a viable replacement of the SC-IM scheme for low-complexity applications, such as internet of things (IoT).

### ACKNOWLEDGMENT

This work was supported by the Natural Science Foundation of China under Grant No. 61671395 and 61871337.

### REFERENCES

- [1] R. Mesleh, H. Haas, C. W. Ahn, and S. Yun, "Spatial modulation - a new low complexity spectral efficiency enhancing technique," in *Proc. Conf. Comm. and Networking in China*, Oct. 2006, Beijing, China, pp. 1-5.
- [2] R. Mesleh, H. Haas, S. Sinanovic, C. W. Ahn, and S. Yun, "Spatial modulation," *IEEE Trans. Veh. Technol.*, vol. 57, no. 4, pp. 2228-2241, July 2008.
- [3] R. Abu-Alhiga and H. Haas, "Subcarrier-index modulation OFDM," in *Proc. 20th IEEE Int. Symp. Personal, Indoor and Mobile Radio Commun.*, Sept. 2009, Tokyo, Japan, pp. 177181.
- [4] D. Tsonev, S. Sinanovic, and H. Haas, "Enhanced subcarrier index modulation (SIM) OFDM," in *Proc. IEEE GLOBECOM Workshops (GC Wkshps)*, Dec. 2011, Houston, TX, USA, pp. 728732.
- [5] E. Basar, U. Aygl, E. Panayirci, and H. V. Poor, "Orthogonal frequency division multiplexing with index modulation," *IEEE Trans. Signal Process.*, vol. 61, no. 22, pp. 5536-5549, Nov. 2013.
- [6] G. Kaddoum, M. F. Ahmed, and Y. Nijssure, "Code index modulation: A high data rate and energy efficient communication system," *IEEE Commun. Lett.*, vol. 19, no. 2, pp. 175-178, Feb. 2015.
- [7] W. Xu, Y. Tan, F. C. M. Lau, and G. Kolumban, "Design and optimization of differential chaos shift keying scheme with code index modulation," *IEEE Trans. Commun.*, vol. 66, no. 5, pp. 1970-1980, May 2018.
- [8] S. Sugiura, S. Chen, and L. Hanzo, "Coherent and differential space-time shift keying: A dispersion matrix approach," *IEEE Trans. Commun.*, vol. 58, no. 11, pp. 3219-3230, Nov. 2010.
- [9] S. Sugiura, S. Chen, and L. Hanzo, "A universal space-time architecture for multiple-antenna aided systems," *IEEE Commun. Surveys Tuts.*, vol. 14, no. 2, pp. 401-420, 2nd Quart., 2012.
- [10] E. Soujeri, G. Kaddoum, M. Au, and M. Herceg, "Frequency index modulation for low complexity low energy communication network," *IEEE Access*, vol. 5, pp. 23276-23287, 2017.
- [11] N. Ishikawa, S. Sugiura, and L. Hanzo, "Subcarrier-index modulation aided OFDM - Will it work?" *IEEE Access*, vol. 4, pp. 2580-2593, 2016.
- [12] H. Sari, G. Karam, and I. Jeanclaude, "Transmission techniques for digital terrestrial TV broadcasting," *IEEE Commun. Mag.*, vol. 33, no. 2, pp. 100109, Feb. 1995.
- [13] M. Nakao, T. Ishihara, and S. Sugiura, "Single-carrier frequency-domain equalization with index modulation," *IEEE Commun. Lett.*, vol. 21, no. 2, pp. 298-301, Feb. 2017.
- [14] D. E. Knuth, *The Art of Computer Programming*. Addison-Wesley, 2005, vol. 4, Fascicle 3, ch. 7.2.1.3.
- [15] J. D. McCaffrey, "Generating the  $m^{th}$  lexicographical element of a mathematical combination," MSDN Library, Jul. 2004. [Online]. Available: [http://msdn.microsoft.com/en-us/library/aa289166\(VS.71\).aspx](http://msdn.microsoft.com/en-us/library/aa289166(VS.71).aspx)
- [16] M. Nakao, T. Ishihara, and S. Sugiura, "Dual-mode time-domain index modulation for Nyquist-criterion and faster-than-Nyquist single-carrier transmissions," *IEEE Access*, vol. 5, pp. 27659-27667, Dec. 2017.